

# AN OVERVIEW FOR SIMULATING THE BLOW OUT OF OIL SPILLS WITH A THREE-DIMENSIONAL MODEL APPROACH (CARIBBEAN COAST, COLOMBIA)

P. C. Leitão • M. S. Malhadas • J. Ribeiro • J. C. Leitão • J. Pierini • L. Otero

## CHAPTER SYNOPSIS

### Background

Oil spill modelling studies are usually focused in the first meters of the sea surface and consequently use a bi-dimensional (2-D) approach. The oil accidents are commonly associated with surface operations (e.g., ship accident, harbor activities) even in the case of blow ups in deep ocean majority of the oil released rise quickly to the surface. However, the works conducted in the DeepSpill Project show that for deep water blowouts dissolution potential of water-soluble oil components in seawater is an important factor when considering potential ecotoxicological effects from acute releases [1]. This is particularly relevant in connection to underwater releases.

In 2010, the Deepwater Horizon (DH) oil spill disaster (also referred to as the BP oil spill, the Gulf of Mexico oil spill, the BP oil disaster, or the Macondo blowout), trigger a great variety of in situ and remotely sensed observations and laboratory and numerical model studies on the oceanographic conditions in the gulf and their influence on the distribution and fate of the discharged oil [2]. One of the studies main focuses was the far-field subsurface and surface dispersal of different size classes of oil released from the DH. In the present work, a similar approach to the one presented in [3] is followed. A 3D coupled hydrodynamic and Lagrangian model system (MOHID) in the Caribbean Coast (Colombia) was applied.

### Results

The 2-D model results show that the horizontal dispersion of oil spills at the surface is governed by wind, waves and surface currents. The oil thickness and track patterns depend on the oceanographic conditions of the simulated period. In case of extreme conditions, particularly persistent winds from the Northwest and West sectors, the oil plume could reach the Caribbean Coast Region and stay trapped along the shoreline of Rosario Islands.

The simulated droplet trajectories of the 3-D model at the Caribbean platform showed that droplets with a diameter of  $50\ \mu\text{m}$  formed a distinct subsurface plume, which was transported horizontally and could remain below the surface. This plume could have a very restricted area of impact because the dispersion is only controlled by the ocean currents which, at 1000 m depth, have a low intensity and are quite turbulent. In this case, the formed plume stayed trapped at 1000 m depth, not posing a risk to the Caribbean Coast. In contrast, droplets with diameters of  $250\ \mu\text{m}$ , 1 and 10 mm rose rapidly to the surface, even with different velocities ( $6, 10, 20\ \text{m s}^{-1}$ ).

### Conclusions

Future oil-spill response models could use this approach to provide real-time forecasts of subsurface oil movement, and ongoing and planned improvements to this coupled model system will likely improve its predictive capabilities.

## 1 INTRODUCTION

The transport and fate of spilled oil in bodies of water are governed by physical, chemical, and biological processes that depend on the oil properties, hydrodynamics, meteorological and environmental conditions [4]. The processes include advection, turbulent diffusion, surface spreading, evaporation, dissolution and emulsification, and may influence the transport of the oil spill. When liquid oil is spilled on the sea surface, it spreads and forms a thin film,

the so-called oil slick [5]. Hence, oil spill models play a significant role in assessing risks and injuries to natural resources from actual and potential spills, and guiding the development of strategies for oil spill planning and response [6].

In spite of a great number of models available for oil spill simulation, most of them traditionally use the semi-empirical [7, 8] and are suitable mainly for oil slick tracking, evaluation of evaporation and generalized oil mass losses due to weathering [9]. The new generation of the models has the ability to predict entrainment, subsurface transport and resurfacing of spilled oil [10, 11].

In the last three decades, many investigators have studied the transport and fate processes of oil spills based on the trajectory method [4, 12-19]. Such models have typically been two-dimensional surface models using constant or variable parameters to link wind and current velocities to the velocity of the surface oil slick [6]. Among these oil spill models, many of them focus on the surface movement of oil spills, since the traditional oil spill models have been used to describe horizontal plane dispersion [5]. Field, laboratory, and modelling studies [19-21] have clearly demonstrated the importance of the vertical dimension in oil movement. These studies have demonstrated that natural entrainment of oil can play an important role not only in mass balance calculations, but also in determining the spatial and temporal distribution of oil on the sea surface [6].

There has been little published research on the vertical distribution of oil but is well known that droplets of higher buoyancy spend proportionately more time on the surface layers and are advected further due to the surface currents than that smaller droplets [5, 3]. The spreading of the oil slick is a three-dimensional (3-D) process controlled by the droplet size distribution and shear diffusion processes [5, 3].

In this case of study the MOHID model was applied to the Caribbean Coast Region for simulating an oil spill associated with a blow out at 1000 m depth scenario. Two different model implementations were undertaken according to the processes addressed: i) horizontal transport at the surface and ii) vertical mixing of oil droplets. The first one is a two-dimensional numerical model application and have the main objective of simulating the transport and fate of the oil fraction able to rise quickly to the surface. This is based on the particle tracking model approach assuming that the amount of oil released is distributed among a large number of particles tracked individually. In a second stage, a Lagrangian discrete particle algorithm has been developed and applied to simulate movement of oil droplets in depth. This application is three-dimensional and consists of predicting vertical mixing assuming different size classes of oil droplets over time.

Performed simulations intend to understand the impact of an oil spill in protected areas along the Caribbean Coast (Rosario and Catalina Island), thus the importance of a 2-D or a 3-D model approach.

## 2 MATHEMATICAL MODEL

MOHID Water Modeling System, an integrated modelling tool, was applied to the study area. The hydrodynamic module of MOHID calculates and updates the flow information sol-

ving the primitive Navier–Stokes equations in the three-dimensional space for incompressible fluids and it is well described by [22]. The hydrodynamic information necessary to calculate the oil trajectories is then passed to the Lagrangian transport model, which computes their spatial evolution using the definition of velocity [23]. The oil weathering module (OWM) uses variables from the hydrodynamics and the Lagrangian transport module, and computes oil density, viscosity, and the weathering processes originally developed by [24].

For this particularly study was added a new vertical velocity component to the oil particles entitle buoyant velocity based in the formulation presented in [5].

## 2.1 Vertical mixing of oil droplets

The buoyant velocity of oil droplets is determined by their size, seawater viscosity and the density difference between seawater and oil droplets [4]. The critical diameter of oil droplets is calculated by the formula [25]:

$$d_c = \frac{(9.52\nu)^{\frac{2}{3}}}{g^{\frac{1}{3}} \left(1 - \rho_0/\rho_w\right)^{\frac{1}{3}}} \quad (1)$$

For small oil droplets  $d_i < d_c$ , Stokes law gives the steady buoyancy velocity depicted in Eq. 2:

$$u_{LS} = gd_i^2 \frac{\left(1 - \rho_0/\rho_w\right)^{\frac{1}{3}}}{18\nu} \quad (2)$$

For large oil droplets  $d_i \geq d_c$ , Reynolds law gives the steady buoyancy velocity showed in Eq. 3:

$$u_{LR} = \sqrt{\frac{8}{3}gd_i \left(1 - \rho_0/\rho_w\right)} \quad (3)$$

Where  $\nu$  is the seawater viscosity, while  $\rho_0$  and  $\rho_w$  are the oil and seawater density, respectively. The rise velocity of droplets can have different orders of magnitude depending on diameters (e.g., for 30 and 300  $\mu\text{m}$  corresponds 0.06 and 6  $\text{mm s}^{-1}$ , respectively). These rise velocities fundamentally control whether the droplets reach the surface, if they form surface plumes (or sub-surface ones), and determine the direction and extent of horizontal dispersal.

For the oil type considered in this work (density = 920  $\text{kg m}^{-3}$ ), and assuming a water density of 1030  $\text{kg m}^{-3}$ , the critical diameter is 210  $\mu\text{m}$  (Figure 1). The velocities for diameters immediately above the critical one are on the order of 2.5  $\text{cm s}^{-1}$  and immediately below on the order of 2.5  $\text{mm s}^{-1}$ . Additionally, the ocean vertical velocities in this area and at this depth vary between 0.5-5  $\text{mm s}^{-1}$ . This means that the droplets with a diameter below the critical diameter will have rising velocities lower or of the same order of magnitude than the environmental velocities, and will have the tendency to be dispersed, mainly due to the action of the ocean currents. The droplets with a diameter above the critical diameter will have rising velocities clearly higher than the hydrodynamic velocities, and will reach the surface quickly.

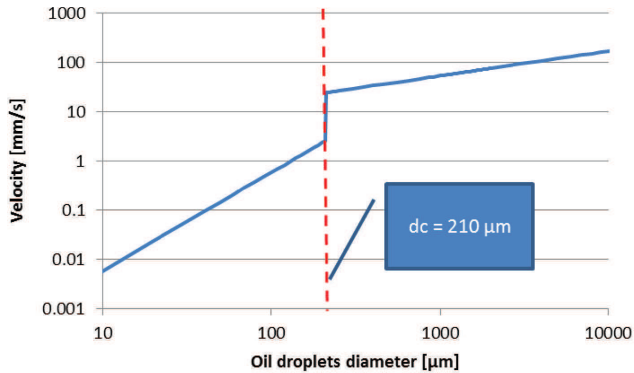


**Figure 1.** Oil droplets rising velocity function of the oil droplets diameter with a  $920 \text{ kg m}^{-3}$  density [4].

### 3 APPLICATION OF THE OIL SPILL MODEL IN THE CARIBBEAN COAST

This section includes a description of 2-D and 3-D oil spill model implementation. The description includes the hydrodynamic and Lagrangian model configurations, model set-up and simulations performed. The 2-D implementation can be considered as the standard used in oil spill studies. The 3-D methodology followed here is similar to the one presented by [3] for the DH Spill.

The main goal of the 3-D model implementation was to illustrate the 3-D behavior of the oil plume in the near field function of the oil droplet dimension. The idea was to validate the hypothesis implicit to the 2-D approach that the plume raises very fast to the surface (order of minutes or a few hours). Another goal was to present a straightforward methodology to downscale a low frequency solution like RTOFS (<http://polar.ncep.noaa.gov/ofs/>) or MyOcean (<http://www.myocean.eu.org/>) [26].

#### 3.1 Study site

The study site of the presumed oil spill (Figure 2, yellow polygon) is located on the Caribbean Coast of Colombia. The coast is about 1600 km long from Castilletes at the western border of Venezuela, to Cabo Tiburón at the eastern border of Panamá. The most important island areas are the coralline archipelagos of El Rosario Islands, 100 km south of Cartagena. The tidal range along the Caribbean Coast is a mixed semi-diurnal type, with maximum amplitudes of 60 cm [27]. The winds predominate from the east, north and northwest at the Guajira Peninsula, and from the northeast to northwest, south of the Sierra Nevada de Santa Marta [28].

The climate of the Caribbean coast is generally characterized by two rainy periods (April-May and October-November) and two dry periods (December-April). Maximum annual precipitation for the Colombian Caribbean does not exceed 2500 mm. Minimum values are within the desert region of the Guajira Peninsula (yearly mean of about 267 mm), and maximum values are at the Sierra Nevada de Santa Marta massif (yearly mean of 2000 mm). Mean air temperatures for the Caribbean coast are less than  $24 \text{ }^{\circ}\text{C}$  [28].

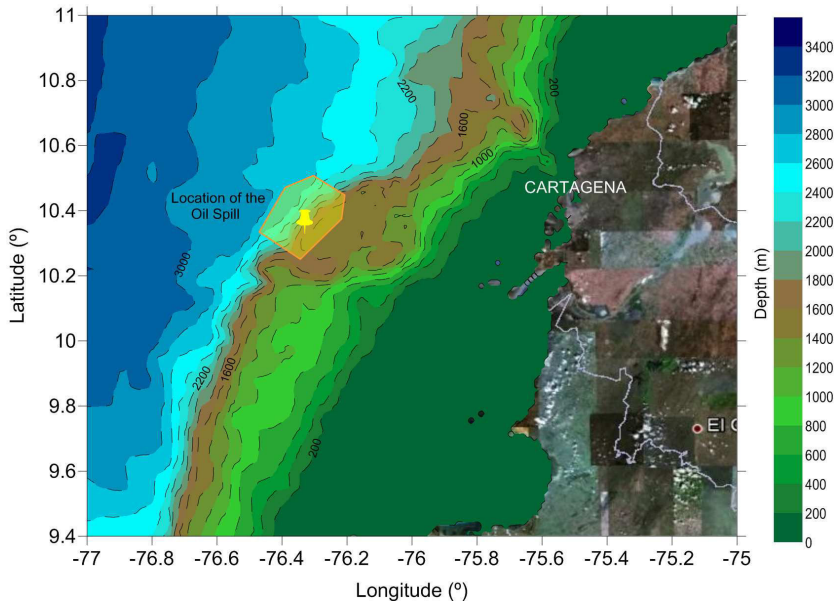


**Figure 2.** Study site: Caribbean coast. Yellow polygon delineates the location considered for the oil spill.

## 3.2 Input data

### 3.2.1 Bathymetries

The bathymetric data used in this study was extracted from the General Bathymetric Chart of the Oceans (GEBCO, <http://www.ngdc.noaa.gov/mgg/gebco/>) and local nautical charts. The main bathymetry characteristics are presented in Table 1 and model domains in Figure 3. The large scale model domain cover the Gulf of Mexico, regional scale the Colombia Coast and local scale Caribbean Coast region.

### 3.2.2 Oceanographic data

The oceanographic data includes wind, surface fluxes, currents, salinity, temperature and waves. The wind and surface fluxes data (temperature, humidity, pressure, solar radiation etc.) for the atmospheric forcing was gathered from NASA World Wind (<http://worldwind.arc.nasa.gov/>) and Global Forecast System (GFS, <http://nomads.nccdc.noaa.gov/>). NASA and GFS model solutions have  $0.22^\circ$  and GFS  $0.5^\circ$  resolution. Both of model predictions have 3-hourly frequency and 7 days forecast. The NASA World Winds solutions were gathered for the periods of January, August, September and November 2008 and GFS for 1 to 9 January 2012.

The currents, salinity and temperature data for the forcing of the hydrodynamic model comes from the Real Time Ocean Forecast System (RTOFS) managed by NOAA (<http://polar.ncep.noaa.gov/ofs/>) based in the Hybrid Coordinate Ocean Model (HYCOM, <http://hycom.org/>). The spatial resolution of the model solutions is about  $1/12^\circ$ . The surface (2-D solution) model predictions have an hourly frequency, while 3-D model solutions have daily one. The forecast extends for 6 days. ROFTS solution was gathered for 1 to 9 January 2012.

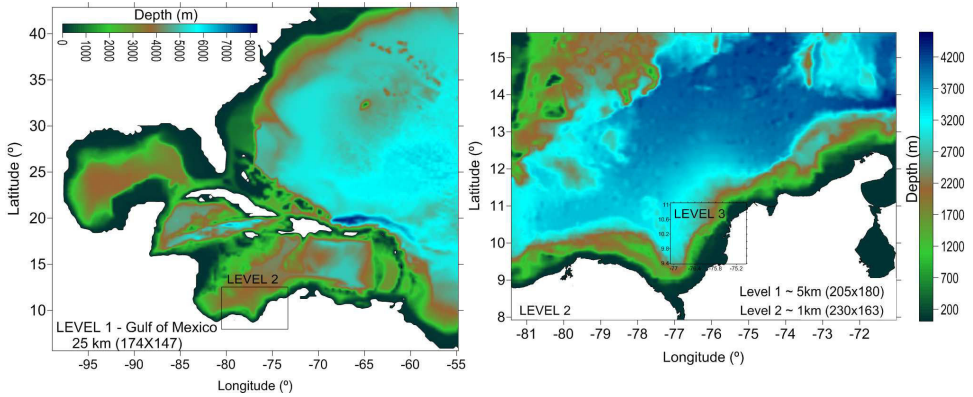


**Figure 3.** Nested domains used in the 2-D and 3-D oil spill model configuration. Gulf of Mexico (large scale model domain) is the level 1, Colombia Coast (regional scale model domain) the level 2 and Caribbean Coast (local scale model domain) level 3.

**Table 1.** Main characteristics of domain bathymetries.

Bathymetry	Coordinates	Dimension (dx/dy)	Resolution (km <sup>2</sup> )
Gulf of Mexico	-99.0° W 5.5° S -54.7° E 42.9° N	174x147	25/0.22
Colombia Coast	-81.4° W 6.5° S -70.9° E 15.7° N	205x180	5/0.045
Caribbean Coast	-77.1° W 9.3° S -74.7° E 11.0° N	230x163	1/0.009

The wave data includes wave peak direction ( $D_p$ ), wave peak period ( $T_p$ ) and significant wave height ( $H_s$ ). This was gathered through operational ocean wave predictions of NOAA/NWS/NCEP with WAVEWATCH III model (<http://polar.ncep.noaa.gov/waves/>). The model domain covers a longitude and latitude of 77° S to 77° N with 1.2°x1° resolution. The model runs on the 00z, 06z, 12z and 18z model cycles, and starts with a 6h hindcast to assure continuity of swell, providing 5 days of forecast. The wave data was downloaded for the periods of January, August, September and November 2008.

### 3.3 Model configuration

#### 3.3.1 2-D oil spill model

The model configuration for the 2-D oil spill model consists of two levels of nested grids (Figure 3): Colombia Coast and Caribbean Coast Region. Colombia Coast has 205x180 cells with 5 kmx5 km of resolution and Caribbean Coast Region a model domain of 230x163 cells with 1 kmx1 km of resolution. The hydrodynamic solution in both grids results from the interpolation of the high frequency (1 hour) RTOFS model surface solution.

Realistic meteorological and wave forcing are included in the model configuration. The wind (intensity,  $\text{m s}^{-1}$  and direction, °N) and wave data ( $D_p$ ,  $T_p$  and  $H_s$ ) were imposed in both nesting levels. Wind data was gathered from the NASA World Winds and wave data from WWIII model solutions.

A Lagrangian transport model was coupled with the hydrodynamic model to simulate the oil spill. A spill volume of about  $3200 \text{ m}^3$  emitted at constant rate over 1 day is assumed. Particles were released in a continuous stream ( $\sim 0.04 \text{ m}^3 \text{ s}^{-1}$ ) at the location  $-76.33^\circ \text{ W}$ ,  $10.33^\circ \text{ N}$  (Figure 2) starting in the beginning of the simulation and ending after one day. During this period of time, 10,000 particles were released. The oil particle movement takes in consideration the effect of currents, waves and winds. Waves generate a drift velocity (stokes drift), and winds have direct drag effect over the floating oil. Processes such as surface spreading, evaporation, dissolution and emulsification were also simulated. For a detailed description of the MOHID oil spill model, see [23]. The oil type considered has an API of 21.3 and a density of  $920 \text{ kg m}^{-3}$  (for more details, see Table 2).

**Table 2.** *Main characteristics of oil.*

Type	Medium Crude Oil
Spill Rate ( $\text{m}^3/\text{hours}$ )	3200/24
API	21.3
Viscosity (cp)	33
$\sigma$ (dyn/cm)	30
Water retention (%)	70
Emulsification Coefficient ( $\text{s}^{-1}$ )	$10^{-6}$

Eight simulations were conducted, each for a specific period and assuming different forcing. Four of these correspond to real periods and aim to represent the seasonal variability, while the other four are considered as extreme conditions. Seasonality is introduced in the specific period of the input data - dry, wet and transition season. Extreme condition scenarios focus only on wind forcing, varying the intensities and directions according to typical values known in the area. In the scenarios of constant winds a random component of about 10% in the direction of the wind was associated. Model simulations performed in this work are presented in Table 3.

### 3.3.2 3-D oil spill model

To simulate the 3-D dispersion of an oil spill at 1000 depth on the Caribbean Coast, an off-line particle-tracking model using the 3-D hydrodynamic stored predictions was implemented. The off-line design was chosen to focus computational power on running a sufficient number of particles to ensure statistical robustness of model results [3]. The model configuration consists of providing hydrodynamic fields generated by a 3-D MOHID model of Caribbean Coast Region as an input to the Lagrangian model. In a first stage was implemented a 3-D model for predicting the hydrodynamic solution at the Caribbean Coast Region. This was simulated with MOHID model ([www.mohid.com](http://www.mohid.com)) using three levels of nesting (Figure 3): Level 1 (Gulf of Mexico), Level 2 (Colombia Coast) and Level 3 (Caribbean Coast Region).

**Table 3.** *Periods and main characteristics of the simulations performed.*

Scenario ID	Simulation Period	Characteristics	Hydrodynamic conditions	
1	18 to 28 January 2008	Wet Season	Currents Waves Wind	RTOFS WWIII NASA WW
2	17 July to 2 August 2008	Dry Season	Currents Waves Wind	RTOFS WWIII NASA WW
3	1 to 9 September 2008	Transition Season	Currents Waves Wind	RTOFS - NASA WW
4	9 to 20 November 2008	Transition Season	Currents Waves Wind	RTOFS WWIII NASA WW
5	96 hours	Extreme Conditions	Currents Waves Wind	- - North, 10 ms <sup>-1</sup>
6	96 hours	Extreme Conditions	Currents Waves Wind	- - Northwest, 6 ms <sup>-1</sup>
7	96 hours	Extreme Conditions	Currents Waves Wind	- - West, 6 ms <sup>-1</sup>
8	96 hours	Extreme Conditions	Currents Waves Wind	- - Southwest, 10 ms <sup>-1</sup>

The Gulf of Mexico has a dimension of  $174 \times 147$  cells and resolution of 25 km and is a 2-D barotropic model. The sea level was assumed to be equal to the FES2004 tide global solution in the open boundary [29]. As initial conditions, a null free surface gradient and null velocity in all grid points were used. The time step is 240 s and the horizontal eddy viscosity is  $250 \text{ m}^2 \text{ s}^{-1}$ .

The Colombia Coast domain with 5 km x 5 km of resolution and  $205 \times 180$  cell points is a 3-D baroclinic model with 40 Cartesian layers. Open Boundary Conditions (OBCs) were defined as a barotropic radiative condition (sea level and barotropic velocities) adding an exterior (or reference) solution equal to Level 1 plus RTOFS (daily average). In reality, the Level 1 corresponds to the high frequency component of the exterior solution and RTOFS to the low frequency. Salinity and temperature values relaxation (or nudging) along the open boundary are interpolated directly from the RTOFS solution. There is also relaxation to a 3-D velocity field resulting from the interpolation of the RTOFS solution plus the Level 1 velocities. The time step used was 120 s and horizontal eddy viscosity  $50 \text{ m}^2 \text{ s}^{-1}$ .

The Caribbean Coast Region model domain (Level 3) has a model domain of  $230 \times 163$  cells with  $1 \text{ km} \times 1 \text{ km}$  of resolution and is also a 3-D baroclinic model nested in the Colombia Coast domain (Level 2). The same vertical discretization of Level 2 (40 Cartesian layers) was used. For the definition of OBCs, a similar methodology to the one followed in Level 2 was adopted. However, in this case, the barotropic exterior solution is only derived from Level 2, and the relaxation procedure is done for the salinity, temperature and velocity values

interpolated directly from the Level 2 model. In this case, Level 2 already incorporates the high and low frequency components. The time step is 40 s and the horizontal eddy viscosity is  $10 \text{ m}^2 \text{ s}^{-1}$ . This downscaling methodology is described in detail in [26].

The model was run for the period of 6 to 9 January 2012 being the first 6 days of simulation considered as a spin-up. The output includes 3-D fields of temperature, salinity, three components of velocity and sea surface height. An example of surface current velocities predicted by the 3-D Hydrodynamic Colombia Coast model can be found in Figure 4.

The second step consists of implementing the Lagrangian oil spill model. The predicted water level, three components of velocities, salinity, temperature, and diffusivities predicted by hydrodynamic model are interpolated for the grid where the particle model runs. It is assumed that particles were assigned characteristics of oil droplets, including diameter and density. Particles trajectories are tracked in three dimensions using advection, mixing and oil droplet rise velocities.

A continuous release ( $\sim 0.04 \text{ m}^3 \text{ s}^{-1}$ ) with the same oil characteristics described for the 2-D model configuration is assumed (Table 2). Particles were released in a continuous stream at the location  $-76.33^\circ \text{ W } 10.33^\circ \text{ N}$  (Figure 2) at 1000 m depth over the 3 days of simulation. The discharge was connected along the entire simulation with the goal of integrating a larger set of conditions. The idea was to look at the oil plume 3-D structure, and not so much the impact of the blow out. A total of 7,000 particles were released during the simulation.

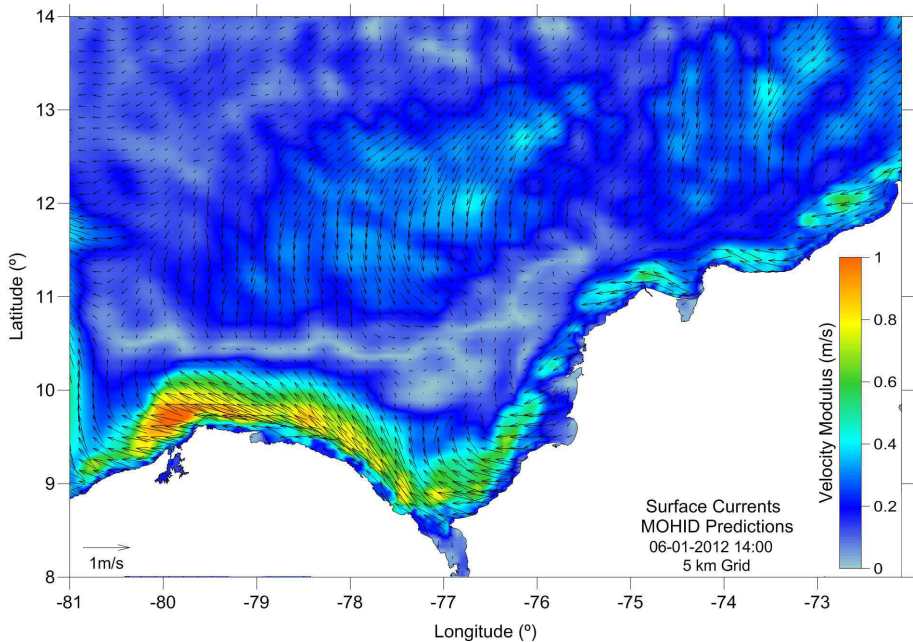


**Figure 4.** Current velocities at the surface predicted by the 3-D hydrodynamic Colombia Coast model on 6 January 2012, 14:00h.

Four simulations for the period of 6 to 9 January 2012 were conducted. The simulations set-up differ according to droplet diameter size and are presented in Table 4. The Lagrangian model input uses the hydrodynamic fields generated by the 3-D MOHID Caribbean Coast Region model. For this hydrodynamic set-up, several oil droplet diameters were simulated: 50 and 250  $\mu\text{m}$ , 1 and 10 mm.

**Table 4.** *Periods and main characteristics of the simulations performed to analyze the vertical transport of oil droplets.*

Scenarios ID	Simulation Period	Droplets diameters	Hydrodynamic conditions	
1	6 to 9 January 2012	50 $\mu\text{m}$	Currents S and T	3-D Mohid Model 3-D Mohid Model
2	6 to 9 January 2012	250 $\mu\text{m}$	Currents S and T	3-D Mohid Model 3-D Mohid Model
3	6 to 9 January 2012	1 mm	Currents S and T	3-D Mohid Model 3-D Mohid Model
4	6 to 9 January 2012	10 mm	Currents S and T	3-D Mohid Model 3-D Mohid Model

## 4 RESULTS AND DISCUSSION

This section presents the most relevant model results obtained with the 2-D and 3-D oil spill model applications. For the 2-D model application, we present the evaporated mass in all scenarios and oil thickness. Results of 3-D model application include particle distributions along vertical depth.

### 4.1 2-D oil spill model

The curves of the evaporated rate in mass obtained for simulated scenarios with a 2-D oil spill model are presented in Figure 5. Results obtained for the scenarios that include seasonal variation in data (Scenario 1- wet season, Scenario 2- dry season, Scenario 3 and 4- transition seasons) are depicted in Figure 5a and different wind forcing (Scenario 5- North, 10  $\text{m s}^{-1}$ , Scenario 6-Northwest, 6  $\text{m s}^{-1}$ , Scenario 7-West, 6  $\text{m s}^{-1}$ , Scenario 6-Southwest, 10  $\text{m s}^{-1}$ ) in Figure 5b.

In general, it is possible to conclude that crude oil reduces about 20-30% of its initial volume in the first 2 days. This reduction is affected mainly by wind, currents and seasonality (e.g., in summer evaporation is higher than that in winter). Figure 5 shows that higher evaporation rates ( $\sim 35\%$ ) are achieved during the dry season simulated scenario, while lesser values are obtained in the others. Simulated scenarios considered wind forcing shows that evaporation rate values occur according to wind intensity (from 6 to 10  $\text{m s}^{-1}$ ). When wind speed increases the evaporation rates tend to be higher (about 30%).

Maximum oil thickness obtained at the surface with the 2-D model for the scenarios that include seasonal variation in data (e.g., Scenario 1- wet season, Scenario 2- dry season, Scenario 3 and 4- transition seasons) is shown in Figure 6 and reveals a different oil slick

pattern for each scenario. This can be explained by the current patterns of each simulated period. The results show a slick separated with relatively thick patterns and different thickness. A maximum thickness between 0.10 and 0.3 mm is predicted by the model, which is in line with other studies (U.S. Department of the Interior, 2006). Areas around oil spill seep slicks tend to be quite thin, with thickness values of about 0.10 mm.

The results of model simulations performed for the scenarios of wind are depicted in Figure 7. These scenarios are considered as extreme scenarios, assuming a situation where the wind is the only forcing. In this situation, a mean intensity and direction considered typical in the study area is assumed.

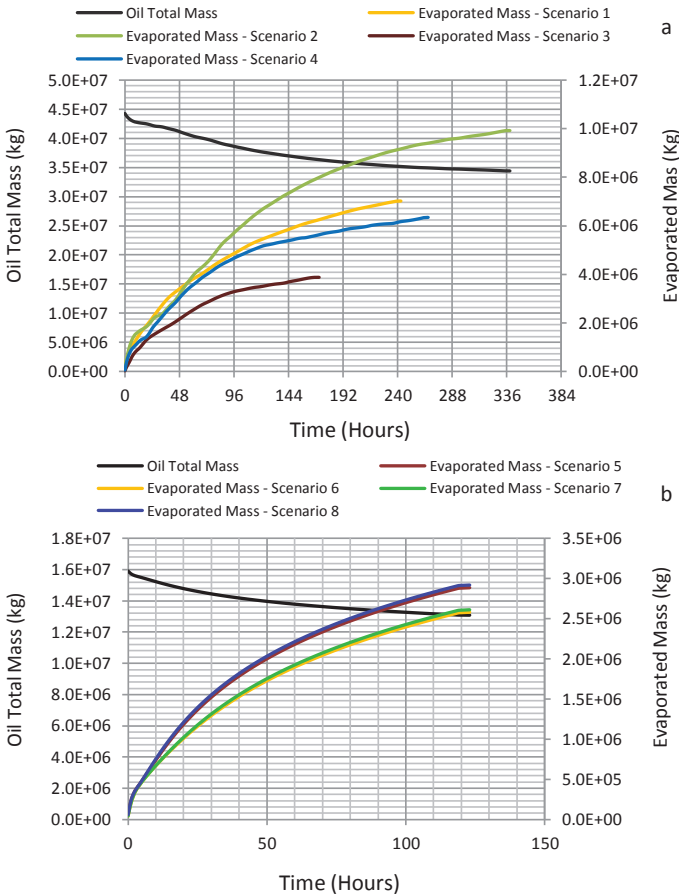


**Figure 5.** Curves of evaporated rate in mass obtained for the scenarios that include a) seasonal variation in data (e.g., Scenario 1 – wet season, Scenario 2 – dry season, Scenario 3 and 4 – transition seasons) and b) different wind forcing (e.g., Scenario 5 – North,  $10 \text{ m s}^{-1}$ , Scenario 6 – Northwest,  $6 \text{ m s}^{-1}$ , Scenario 7 – West,  $6 \text{ m s}^{-1}$ , Scenario 8 – Southwest,  $10 \text{ m s}^{-1}$ ).

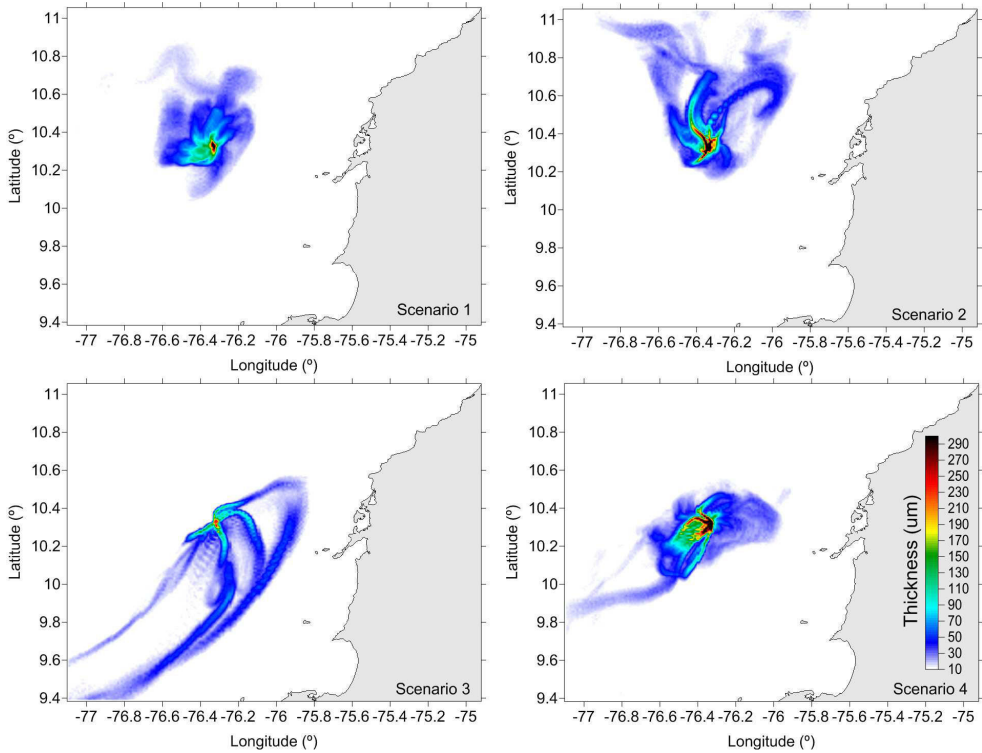


**Figure 6.** Maximum oil thickness obtained at the surface with 2-D model for the scenarios that include seasonal variation in data (e.g., Scenario 1 – wet season, Scenario 2 – dry season, Scenario 3 and 4 – transition seasons).

Simulations performed for the wind scenarios allow an evaluation of the surface oil plume for the areas of interest, Rosario Islands. The results reveal lower values of thickness (about 0.1 mm) when compared with the scenarios presented above. This is explained by the fact that, for these extreme cases, we assume that the only forcing is the wind (no waves and currents). Hence, the oil dispersion is more efficient, generating lower thickness values. Regarding the oil plumes in face of winds scenarios, it can be observed that Northwest and West are the most unfavorable situations. In these cases, the oil spill could reach the coast, and is seized along the coast.

#### 4.2 3-D oil spill model

The particle position predictions for oil droplets sized  $50 \mu\text{m}$  is depicted in Figure 8 (a - shelf front view and b - along shelf view). The same kind of results, but for  $250 \mu\text{m}$ , 1 mm and 10 mm droplet sizes, are shown in Figure 9, Figure 10 and Figure 11.

The model simulations for fixed-diameter particles indicate that oil droplet diameter significantly influenced the transport of oil in water column. The predicted distributions of the particles in depth indicate that two types of plumes could be generated depending on the oil

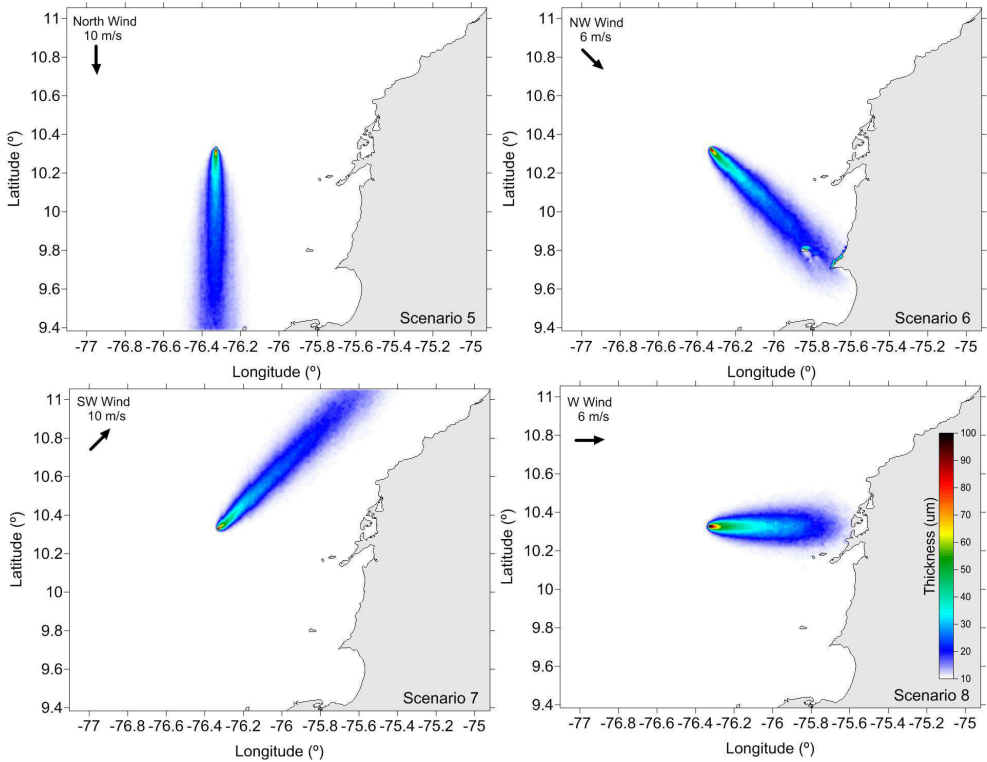


**Figure 7.** Maximum oil thickness obtained at the surface with 2-D model for the scenarios with different wind forcing (e.g., Scenario 5 – North,  $10 \text{ m s}^{-1}$ , Scenario 6 – Northwest,  $6 \text{ m s}^{-1}$ , Scenario 7 – West,  $6 \text{ m s}^{-1}$ , Scenario 8 – Southwest,  $10 \text{ m s}^{-1}$ ).

droplets' size. Particles with diameters of  $50 \mu\text{m}$  have low rising velocities ( $\sim 0.08 \text{ mm s}^{-1}$  vertical velocity) below typical velocities due to local hydrodynamics. In this situation, the sub-surface plume tends to stay trapped around 1,000 m (Figure 8) in depth. The plume tends to disperse through the water column and be transported horizontally (Figure 6) due to physical processes (e.g., tide, internal waves and density currents). The oscillating movement at trapped depth ( $\sim 1,000 \text{ m}$ ) could maintain the plume below surface for a long time (time scales on the order of months). The behavior of this kind of oil droplets is also predicted by the application of the SABGOM-LTRANS model to the Gulf of Mexico [3]. The predictions of the oil plume generated by droplets of  $50 \mu\text{m}$  suggest a small risk for the Caribbean Coast Region. This could be explained by the fact that plumes remain at lower depths ( $\sim 1,000 \text{ m}$ ) for long-time. Additionally, there are oil degradation processes, which in this present version of MOHID are only connected when the oil particles reach the surface.

Particles with diameters of  $250 \mu\text{m}$ , 1 and 10 mm rose quickly to the surface (Figure 9, Figure 10 and Figure 11) with ascending velocities of about 6, 10 and  $20 \text{ cm s}^{-1}$ . The  $250 \mu\text{m}$  particles take around 4 hours to reach surface. In the area of the oil spill, horizontal

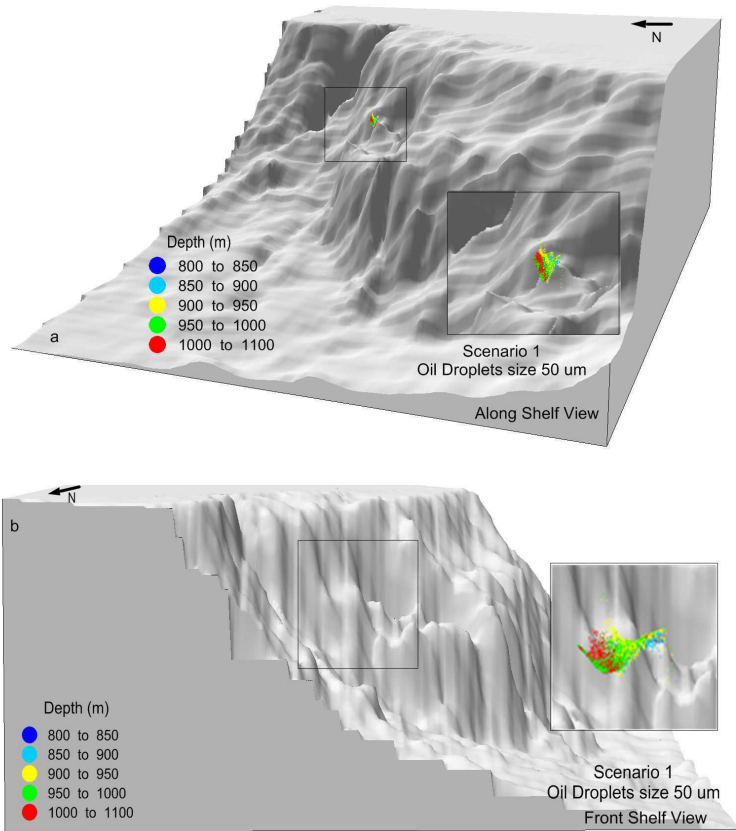


**Figure 8.** Particle position along water depth for Scenario 1 – oil droplets size of  $50 \mu\text{m}$ : a) along shelf view and b) shelf front view.

velocities have typical intensities of  $10 \text{ cm s}^{-1}$ ; this means for the  $250 \mu\text{m}$  oil droplets, there is a horizontal displacement before reaching the surface on the order of 2 km. The analysis of the oil droplet velocity presented earlier (Figure 1) clearly predicts the two types of dispersion described above. For oil droplets with a diameter above  $210 \mu\text{m}$  (critical diameter), the oil will reach the surface quickly. Droplets below the critical diameter would be dispersed mainly by the ocean 3-D current field.

At the surface, the plume is governed mainly by winds, waves and surface currents, and is highly dependent on instantaneous conditions; this means that the 2-D oil spill model is a valid methodology. After reaching the surface, particles remained there and started to be affected by horizontal dispersion induced by currents, winds and waves.

During the predicted time, the plume clearly deviates from the Caribbean Coast Region due to surface currents. However, since the surface plume is controlled by horizontal dispersion processes, as we saw in 2-D model application, in the case of extreme conditions of persistent winds, the oil plume could travel inshore and reach the Caribbean Coast region.

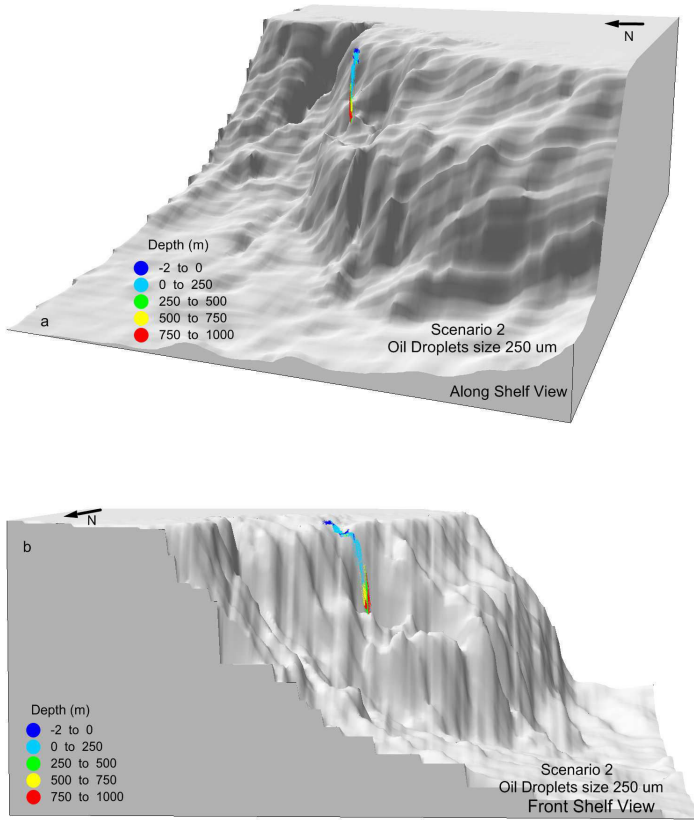


**Figure 9.** Particle position along water depth for Scenario 2 – oil droplets size of  $250 \mu\text{m}$ : a) along shelf view and b) shelf front view.

## 5 CONCLUSIONS

The turbulent zone created at the release point causes the oil to fragment into droplets. Droplet sizes vary as a function of the exit conditions and velocities. Data presented by [30] based on field and laboratory work lead to the conclusion that the majority of the release droplets under a blowout situation have a diameter larger than  $250 \mu\text{m}$  (>90% of the release volume). The same conclusion can be reached based in the DeepSpill project's experimental data [1]. This means that the majority of the oil released will rise quickly to the surface. However, this data should be confirmed with the company responsible for operating the infrastructure related to this study.

In conclusion, it can be stated that, in the case of blow outs, two types of dispersion analyses must be done:

1. Focus on the majority of the released oil (>90%) that reaches surface almost in the same horizontal point of the release depth ( $\sim 2 \text{ km}$  difference). In this case, the traditional 2-D approach is valid;

2. Focus in a small fraction of the released oil (<10%), but which is quite toxic. In this case, the dispersion is mainly controlled by the ocean's 3-D hydrodynamic structure. This means that this oil fraction will be dispersed quite slowly. At the release point, velocities are quite turbulent (do not have clear direction) and are small (horizontally  $5\text{--}50\text{ mm s}^{-1}$  and vertically  $0.5\text{--}5\text{ mm s}^{-1}$ ). This can be clearly seen in the aerial view, side by side plot, of the oil spill plume for the  $50\text{ }\mu\text{m}$  and  $250\text{ }\mu\text{m}$  oil droplet diameter scenarios (Figure 10). The plume associated with  $250\text{ }\mu\text{m}$  oil droplets covers a horizontal area at least two orders of magnitude greater than the  $50\text{ }\mu\text{m}$  scenario. The area of impact of the more dissolved fractions will tend to be restricted. The impact over the web food of these more toxic oil components is the main point of concern.

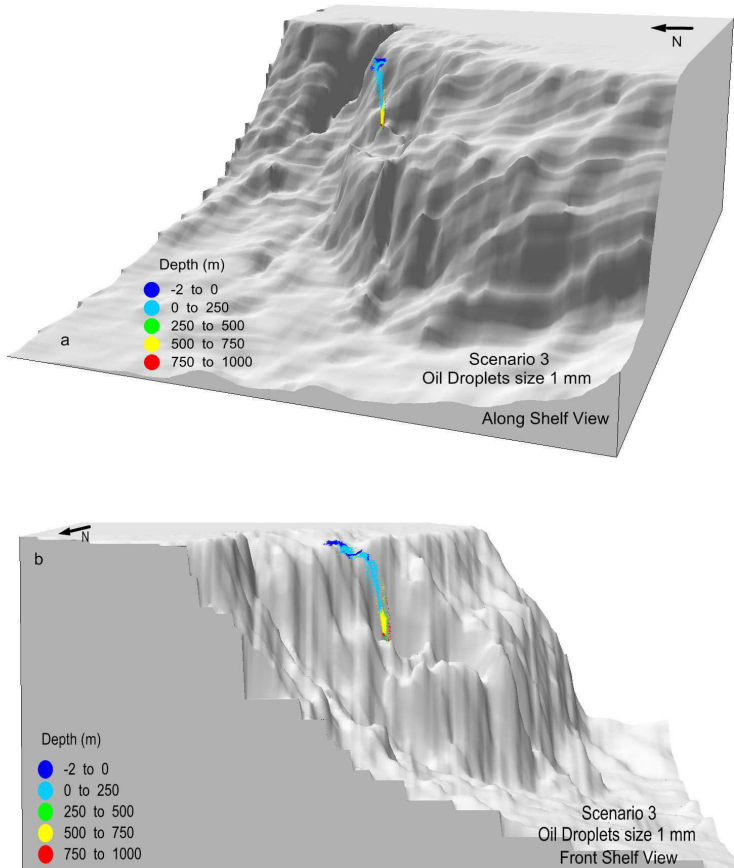


**Figure 10.** Particle position along water depth for Scenario 3 – oil droplets size of 1 mm: a) along shelf view and b) shelf front view.

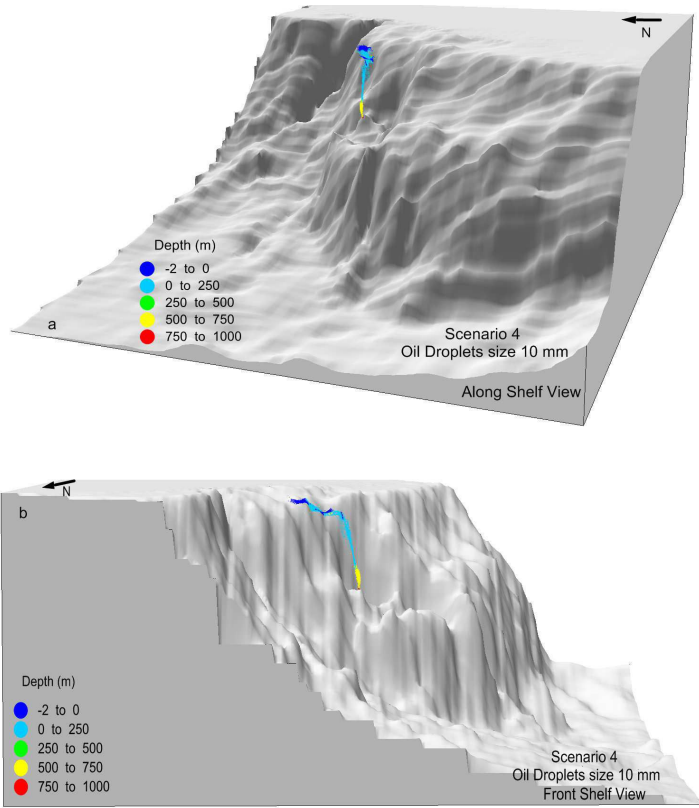


**Figure 11.** Particle position along water depth for Scenario 4 – oil droplets size of 10 mm: a) along shelf view and b) shelf front view.

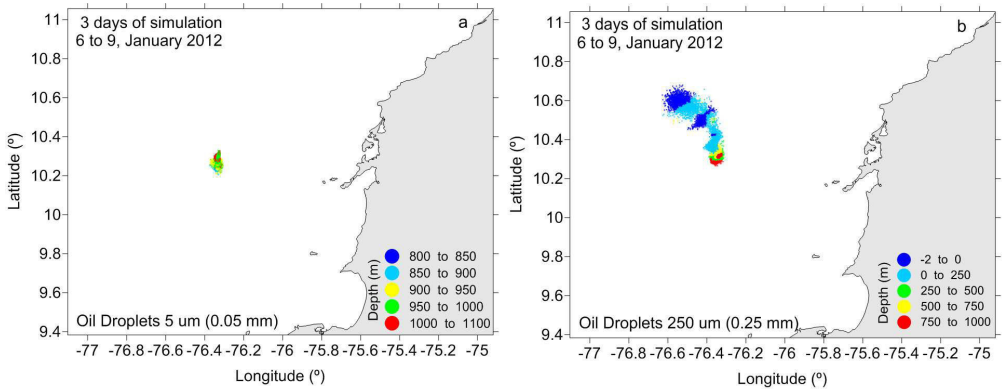


**Figure 12.** Aerial view of the oil plumes after 3 days of simulation: a) 50  $\mu\text{m}$  and b) 250  $\mu\text{m}$ .

## ACKNOWLEDGEMENTS

The authors wish to thank ECOPETROL S.A (Columbian Oil Company) and GEOTEC Ingeniería Ltda.

## REFERENCES

1. Johansen, O., Rye, H., Melbye, A., Jensen, H., Serigstad, B. and Knutsen, T. 2001. Deep Spill JIP Experimental Discharges of Gas and Oil at Helland Hansen, Parts I, II, and III – Technical Report, SINTEF Applied Chemistry, Norway.
2. Liu, Y., A. MacFadyen, Z.-G. Ji, and R. H. Weisberg (Eds.) 2011, Monitoring and Modeling the Deepwater Horizon Oil Spill: A Record-Breaking Enterprise, Geophys. Monogr. Ser., vol. 195, 271 pp., AGU, Washington, D. C., doi:10.1029/GM195.
3. North, E. W., E. E. Adams, Z. Schlag, C. R. Sherwood, R. He, K. H. Hyun, and S. A. Socolofsky 2011, Simulating oil droplet dispersal from the Deepwater Horizon spill with a Lagrangian approach, in Monitoring and Modeling the Deepwater Horizon Oil Spill: A Record-Breaking Enterprise, Geophys. Monogr. Ser., vol. 195, edited by Y. Liu et al., pp. 217–226, AGU, Washington, D. C., doi:10.1029/2011GM001102
4. Wang, S.D., Shen, Y.M., Zheng, Y.H., 2005. Two-dimensional numerical simulation for transport and fate of oil spills in seas. *Ocean Engineering* 32, 1556–1571.
5. Wang, S.D., Shen, Y.M., Zheng, Y.H., Guo, Y.K, Tang, J. 2008. Three-dimensional numerical simulation for transport of oil spills in seas. *Ocean Engineering* 35, 503–510.
6. Reed, M., Turner, C., Odulo, A., 1994. The role of wind and emulsification in modelling oil spill and drifter trajectories. *Spill*.
7. Fay, J.A., 1969. The spread of oil on a calm sea. In: D. Hoult (Ed.), *Oil on the Sea*. Plenum Press.
8. Fay, J.A., 1971. Physical processes in the spread of oil on a water surface. In: Proc. Conf. Prevention and Control of Oil Spills, 15-17 June. American Petroleum Institute, Washington, DC, pp. 463-467.
9. Tkalich P., Huda K., Gin K. 2003. A multiphase oil spill model. *Journal of Hydraulic Research* Vol. 41, No. 2, pp. 115–125.
10. Elliot, A.J., Hurford, N., Penn, C.J., 1986. Shear diffusion and the spreading of oil slicks. *Mar. Pollut. Bull.* 17, 308-313.
11. Spaulding, M.L., 1995. Oil spill trajectory and fate modelling: State-of-the art review. In: *Proceeding of the Second International Oil Spill Research and Development Forum*, IMO, London, UK.
12. Mackay, D., Paterson, S., Nadeau, S., 1980. Calculation of the Evaporation Rate of Volatile Liquids. *Proceedings, National Conference on Control of Hazardous Material Spills*, Louisville, Ky., pp. 364–368.
13. Huang, J.C., Monastero, F.C., 1982. Review of the State-of-the Art of Oil Spill Simulation Models. Final Report Submitted to the American Petroleum Institute, by Raytheon Ocean Systems Co., East Providence, R.I.
14. Shen, H.T., Yapa, P.D., Petroski, M.E., 1986. Simulation of oil slick transport in Great Lakes connecting channels. Report Nos.86–1 to 4, vols. I–IV, Department of Civil and Environmental Engineering, Clarkson University, Potsdam, NY.
15. Shen, H.T., Yapa, P.D., 1988. Oil slick transport in rivers. *Journal of Hydraulic Engineering* 114, 529–543.
16. Yapa, P.D., Shen, H.T., Angamma, K., 1994. Modeling oil spills in a river–lake system. *Journal of Marine System* 4, 453–471.
17. Lonin, S.A., 1999. Lagrangian model for oil spill diffusion at sea. *Spill & Technology Bulletin* 5 (5/6), 331–336.

18. Chao, X.B., Shankar, N.J., Cheong, H.F., 2001. Two- and three dimensional oil spill model for coastal waters. *Ocean Engineering* 28, 1557–1573.
19. Johansen, E., 1984. The Halten Bank experiment observations and model studies of drift and fate of oil in the marine environment. In: *Proceedings of the 11th Arctic Marine Oil Spill Program (AMOP) Techn. Seminar*. Environment Canada, pp. 18-36.
20. Delvigne, G.A.L., Sweeney, C.E., 1988. Natural dispersion of oil. *Oil and Chemical Pollution* 4, 281-310.
21. Singasaas, I., Daling, P.S., 1992. Meso-scale test for laboratory weathering of oil. In: *Proceedings of the 158th Arctic and Marine Oil Spill Program Technical Seminar*, Environment Canada, pp. 55-66.
22. Martins, F., Leitão, P., Silva, A., Neves, R., 2001. 3D modelling in the sado estuary using a new generic vertical discretization approach. *Oceanologica Acta* 24, S51–S62.
23. Janeiro J, Fernandes E, Martins F, Fernandes R. Wind and freshwater influence over hydrocarbon dispersal on Patos Lagoon, Brazil. *Marine Pollution Bulletin*. 2008; 56(4): 650-665.
24. Fernandes, R., 2001. Modelação de derrames de hidrocarbonetos. Trabalho de Final de Curso (Graduation Thesis). Relatório Final. Instituto Superior Técnico, Portugal.
25. Lou, A.G., Wu, D.X., Wang, X.C., Xi, P.G., 2001. Establishment of a 3-D model for oil spill prediction. *Journal of Ocean. University of Qingdao* 31 (4), 473–479 (in Chinese).
26. Leitão P, Coelho H, Santos A, Neves R. Modelling the main features of the Algarve coastal circulation during July 2004: A downscaling approach. *Journal of Atmospheric & Ocean Science*. 2005; 10(4): 421-462.
27. Tuchkovenko, Y.S. and Calero, L.A, 2003. Mathematical modelo of the Ciénaga Grande de Santa Marta Ecosystem. *Bol. Invermar* 2003, vol.32, n.1, pp. 145-167. ISSN 0122-9761.
28. IGAC, 2002. 7th Scientific Conference of the International Global Atmospheric Chemistry Project. 18-25 September 2002 Crete, GREECE.
29. Lyard, L., F. Lefevre, T. Letellier and O. Francis, 2006: Modelling the global ocean tides: modern insights from FES2004. *Ocean Dyn.*, 56, 394-415.
30. Ross, S. L. Environmental Research Ltd., Fate and Behavior of Deepwater Subsea Oil Well Blowouts in the Gulf of Mexico. Minerals Management Service, 1997.